

**VISCOELASTIC EVOLUTION OF LUNAR MULTI-RING BASINS.** P. S. Mohit<sup>1</sup> and R. J. Phillips<sup>1</sup>, <sup>1</sup>Dept. of Earth and Planetary Sciences & McDonnell Center for the Space Sciences, Washington University, St. Louis, MO 63130 USA ([pmohit@wustl.edu](mailto:pmohit@wustl.edu), [phillips@wustite.wustl.edu](mailto:phillips@wustite.wustl.edu))

**Introduction:** Multi-ring basins on the Moon provide a window into early lunar thermal history. Most of the oldest basins are highly degraded and have little topographic expression. This has typically been explained by relaxation of relief through viscous flow of the crust and mantle on geologic timescales [1]. However, the great age of these basins also allows the possibility that they formed when the lunar crust was very hot or partially molten, facilitating enhanced crater collapse during formation or very rapid relaxation [2,3]. Any successful hypothesis for basin evolution must explain why South Pole-Aitken basin (SPA), believed to be the oldest and largest impact basin on the Moon, has retained high-amplitude topographic relief. Here we determine the conditions necessary to produce viscous relaxation and discuss the implications of these results for lunar thermal history.

**Lunar Basins:** Table 1 lists the basins considered in this study and some of their relevant properties. Fig. 1 displays the basins on a plot of free-air gravity vs. basin depth, revealing three basic groups. Group 1 basins (blue) are the best-preserved, showing the greatest depths and little mare fill. Group 2 basins (red) have been filled with large quantities of mare basalt and are characterized by flat floors, reduced depths, and high-amplitude free-air anomalies. Group 3 basins (yellow), among the oldest on the Moon, have little or no topographic relief and low-amplitude free-air and Bouguer anomalies, consistent with viscous relaxation. It has been proposed that the crustal structure of the mascon basins (Groups 1 and 2 here) resulted from the collapse of the transient cavity [4,5], which is consistent with geophysical and numerical studies of the structure of the terrestrial Chicxulub basin [6,7]. It follows that if the degraded state of a Group 3 basin is the result of viscous relaxation, a Group 1 basin of comparable size should likely provide a good approximation of its initial structure, post impact. Fig. 2 shows the Group 1 basin Mendel-Rydberg (M-R) as an example, created from an updated crustal thickness inversion of [8] that employs a thinner crustal thickness constraint (31 km) at the Apollo 12 and 14 sites (M. Wieczorek, pers. comm.).

**Model:** To examine basin relaxation quantitatively, we use a semi-analytic, self-gravitating viscoelastic relaxation model based on the methods of [9,10,11,12]. We solve the continuity, conservation of momentum, and Poisson equations for a viscoelastic spherical body.

We approximate a non-Newtonian rheology by several constant viscosity layers. The viscosity of each layer is determined using a simple thermal model [13] and the flow law of dry diabase [14]. To account for the thinned crust beneath the basin, we set the viscosity of the region extending from the depth of maximum Moho uplift to the base of the background crust equal to the viscosity at the top of this interval. The thermal model consists of a megaregolith extending to a depth of ~2 km, with a thermal conductivity ( $k_{MR}$ ) of 0.2 W/m·K, and bedrock with  $k_{BR} = 2.6$  W/m·K beneath. We parameterize the models using the temperature at the base of the crust ( $T_b$ ), the crustal thickness ( $T_c$ ), and the radiogenic heat production in the crust ( $H$ ).

**Results:** We investigate the evolution of lunar basins using the crustal structure of Group 1 basins to represent the initial condition. Due to the relative weakness of the crust compared to the mantle, we find, not surprisingly, that the relaxation time increases with decreasing crustal thickness and increasing basin diameter. Due to the elastic strength of the upper crust (and to membrane support for the larger basins), a fraction of the surface topography is supported by the lithosphere and tends not to relax completely on geologic timescales. This fraction increases with increasing lithospheric thickness. The presence of a high abundance of radioactive elements in the crust thins the lithosphere and facilitates relaxation. The results are summarized in Table 2 as a function of basin size and  $T_c$ . For  $T_c = 45$  km, applicable to Tsiolkovsky-Stark (T-S) and Keeler-Heaviside (K-H),  $T_b \geq 1300$  K ( $q \geq 40$  mWm<sup>-2</sup> into the base of the crust) is required for complete relaxation to occur in  $\sim 10^8$  yr. Figure 3 shows the evolution of a basin originally like M-R under these conditions. The long wavelengths relax almost completely, leaving a basin dominated by short wavelength topography. Both the amplitude and wavelength of the model topography resemble those of K-H and T-S, supporting the hypothesis that they have relaxed. On the nearside, the crust is significantly thinner (25–35 km), requiring at least near-solidus temperatures at the crustal base to permit basin relaxation by lower crustal flow. In the Procellarum KREEP Terrane (PKT), where the crust is thinnest, super-solidus temperatures and/or high concentrations of heat producing elements would be necessary and might be expected because of the concentration of heat producing elements in this region [15]. SPA's very thin crust (see Table 1) imposes similar conditions; its relatively well-

preserved topography suggests that these conditions were not met.

**Discussion and Conclusions:** The results show that viscous relaxation is a plausible explanation for the degraded state of many lunar basins and allow us to place constraints on temperatures in the lower lunar crust at the times of formation. When the oldest basins formed, the lower crust must still have been ductile, which suggests temperatures  $> 1300$  K at its base and  $q \geq 40$  mWm $^{-2}$ . Basins located in regions of unusually thick crust would be able to relax at lower temperatures ( $q \geq 30$  mWm $^{-2}$ ). Conversely, basins that formed in the thin nearside crust require at least near-solidus conditions at the base of the crust and may have formed during or shortly after the crystallization of the magma ocean. In the PKT, super-solidus conditions or high concentrations of radioactive elements would be required, which is consistent with thermal evolution models of the region [15]. Under these extreme conditions, immediate structural collapse or accelerated relaxation may also be a factor. That SPA has not relaxed despite its great age suggests that similar conditions did not exist on the farside at the time of its formation. These results, combined with the dearth of mare volcanism on the farside and the high concentration of radiogenic elements in the PKT, suggest that the farside cooled faster than the nearside. This thermal asymmetry might have occurred as a consequence of the crustal thickness asymmetry. Once the magma ocean had mostly cooled, the remaining liquid would tend to pool beneath the thin crust of the nearside, bringing with it the majority of the heat-producing elements. Further cooling would then have sequestered the dregs into the PKT.

**References.** [1] Solomon, S.C. et al., *JGR* 87, 3975-3992, 1982. [2] Schenk, P.M., *Nature* 417, 419-421, 2002. [3] Turtle, E. P., B.A. Ivanov, *LPSC* 33, abstr. 1431, 2002. [4] Neumann, G.A. et al., *JGR* 101, 16,841-16,843, 1996. [5] Wieczorek, M.A., R.J. Phillips, *Icarus* 139, 246-259, 1999. [6] Morgan, J.V. et al., *EPSL* 183, 347-354, 2000. [7] Collins, G.S. et al., *Icarus* 157, 24-33, 2002. [8] Wieczorek, M.A., R.J. Phillips, *JGR* 103, 1715-1724, 1998. [9] Grimm, R.E., S.C. Solomon, *JGR* 93, 11,911-11,929, 1988. [10] Grimm, R.E., R.J. Phillips, *JGR* 96, 8305-8324, 1991. [11] Richards, M.A., B.H. Hager, *JGR* 89, 5987-6002, 1984. [12] Zhong, S., M.T. Zuber, *JGR* 105, 4153-4164, 2000. [13] Warren, P.H., K.L. Rasmussen, *JGR* 92, 3453-3465, 1987. [14] Mackwell, S.J. et al., *JGR* 103, 975-984, 1998. [15] Wieczorek, M.A., R.J. Phillips, *JGR* 105, 20417-20430, 2000. [16] Spudis, P.D., *The geology of multi-ring impact basins*, Cambridge University Press, Cambridge, UK, 1993. [17] Wilhelms, D.E., *USGS Prof. Paper* 1348, 1987. [18] Halekas, J.S., R.P. Lin, D.L. Mitchell, *M&PS* 38, 565-578, 2003.

	M-R	Ori	SPA
$T_c = 60$ km	30	35	40
$T_c = 45$ km	40	45+	45+
$T_c = 30$ km	55+	55+	55+

Table 2- Heat flux (in mWm $^{-2}$ ) required for relaxation for three basin sizes. A "+" indicates that sub-solidus relaxation does not occur.

Basin	D (km)	Age	$T_c^{\min}$ (km)	Grp
South Pole-Aitken (SPA)	2500	P-14	6	1
Imbrium (Imb)	1160	I-3	13	2
Crisium (Cri)	1060 (740 $^*$ )	N-4	3	2
Fecunditatis (Fec)	990	P-13	21	3
Orientale (Ori)	930	I-1	8	1
Australe (Aus)	880	P-13	35	3
Nectaris (Nec)	860	N-6	6	2
Smythii (Smy)	840 (740 $^*$ )	P-11	7	2
Humorum (Hum)	820 (425 $^*$ )	N-4	9	2
Tranquilitatis (Tra)	800 (700 $^*$ )	P-13	35	3
Serenitatis (Ser)	740 (920 $^*$ )	N-4	9	3
Mutus-Vlacq (M-V)	700 $^*$	P-13	29	3
NW Procellarum (NWP)	700	P	25	3
Tsiolkovsky-Stark (T-S)	700	P-14	50	3
Nubium (Nub)	690	P-13	24	3
Mendel-Rydberg (M-R)	630 (420 $^*$ )	N-6	20	1
Lomonosov-Fleming (L-F)	620 #	P-13	33	3
Humboldtianum (Hmb)	600 (650 $^*$ )	N-4	8	2
Freundlich-Sharonov (F-S)	600	P-8	21	1
Hertzsprung (Her)	570	N-4	49	1
Coulomb-Sarton (C-S)	530 (440 $^*$ )	P-11	30	1
Balmer (Bal)	500 $^*$	P	28	3
Keeler-Heaviside (K-H)	500 $^*$	P-12	45	3
Korolev (Kor)	440	N-6	58	1
Moscoviense (Mos)	440 (420 $^*$ )	N-6	17	1
Grimaldi (Gri)	430 (440 $^*$ )	P-7	27	2

Table 1- List of the major lunar basins. Locations are from [4,16], diameters (D) from [4], [16] (denoted by \*), and [17] (#). Relative ages are assigned following [18]; I = Imbrian, N = Nectarian, P = pre-Nectarian, and greater numbers indicate greater age.  $T_c^{\min}$  is the minimum crustal thickness, in the center of the basin [8, updated].

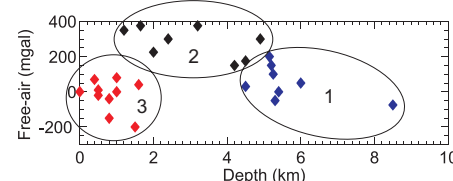


Figure 1. Plot of free-air anomaly amplitude vs. basin depth. The ovals indicate the three groups of basins.

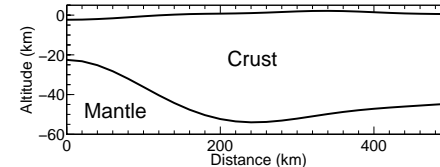


Figure 2. Crustal structure of Mendel-Rydberg.

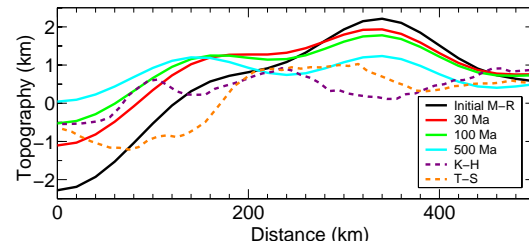


Figure 3. Model evolution of Mendel-Rydberg over time for  $T_c = 45$  km and  $T_b = 1300$  K. Keeler-Heaviside (K-H) and Tsiolkovsky-Stark (T-S) basin profiles shown for comparison.